THE JOURNAL OF BIOLOGICAL CHEMISTRY VOL. 281, NO. 5, pp. 2882–2892, February 3, 2006

HMA1, a New Cu-ATPase of the Chloroplast Envelope, Is Essential for Growth under Adverse Light Conditions*[S]

Received for publication, July 29, 2005, and in revised form, October 26, 2005 Published, JBC Papers in Press, November 10, 2005, DOI 10.1074/jbc.M508333200

Daphné Seigneurin-Berny[‡1,2], Antoine Gravot[§1], Pascaline Auroy[§], Christophe Mazard[‡], Alexandra Kraut[‡], Giovanni Finazzi[¶], Didier Grunwald[‖], Fabrice Rappaport[¶], Alain Vavasseur[§], Jacques Joyard[‡], Pierre Richaud[§], and Norbert Rolland[‡3]

From the [‡]Laboratoire de Physiologie Cellulaire Végétale, Unité Mixte de Recherche (UMR) 5168 CNRS/CEA/Institut National de la Recherche Agronomique, Université Joseph Fourier, Département Réponse et Dynamique Cellulaires (DRDC)/CEA-Grenoble, 17 rue des Martyrs, 38054 Grenoble-cedex 9, France, the [§]Laboratoire des Echanges Membranaires et Signalisation, UMR 6191 CNRS/CEA/Université Aix-Marseille II, Département d'Ecophysiologie Végétale et de Microbiologie/CEA Cadarache, 13108 St Paul les Durance Cedex, France, the [¶]Institut de Biologie Physico-Chimique, UMR 7141 CNRS/Université Paris 6, 13 rue P. et M. Curie, 75005 Paris, France, and the [‖]Laboratoire Canaux Ioniques, Fonctions et Pathologies, EMI 9931 CEA/INSERM/Université Joseph Fourier, DRDC/CEA-Grenoble, 17 rue des Martyrs, 38054 Grenoble-cedex 9, France

Although ions play important roles in the cell and chloroplast metabolism, little is known about ion transport across the chloroplast envelope. Using a proteomic approach specifically targeted to the *Arabidopsis* chloroplast envelope, we have identified HMA1, which belongs to the metal-transporting P_{1B}-type ATPases family. HMA1 is mainly expressed in green tissues, and we validated its chloroplast envelope localization. Yeast expression experiments demonstrated that HMA1 is involved in copper homeostasis and that deletion of its *N*-terminal His-domain partially affects the metal transport. Characterization of *hma1 Arabidopsis* mutants revealed a lower chloroplast copper content and a diminution of the total chloroplast superoxide dismutase activity. No effect was observed on the plastocyanin content in these lines. The *hma1* insertional mutants grew like WT plants in standard condition but presented a photosensitivity phenotype under high light. Finally, direct biochemical ATPase assays performed on purified chloroplast envelope membranes showed that the ATPase activity of HMA1 is specifically stimulated by copper. Our results demonstrate that HMA1 offers an additional way to the previously characterized chloroplast envelope Cu-ATPase PAA1 to import copper in the chloroplast.

Chloroplasts contain a large variety of ions among which metal ions such as copper, iron, manganese, and zinc that are essential for their development and function. Copper is an essential redox cofactor required for a wide variety of processes, including photosynthetic electron transfer reactions (plastocyanin) and detoxification of superoxide radicals (Cu/Zn-superoxide dismutase, SOD)[4] (1). Other metal ions are cofactors for several enzymatic reactions: zinc is associated with chloroplast SOD, methionine synthase, carbonic anhydrase; manganese is required for oxygen evolution in photosynthesis; whereas iron is a cofactor of iron SOD and is found in iron-sulfur clusters of cytochrome b_6f complex, ferredoxin, photosystem I (PSI), and photosystem II (PSII) (2). All these metals are essential micronutrients but are toxic when present in excess (3). To maintain the concentration of metals within physiological limits, cells possess mechanisms that control the uptake, accumulation, trafficking, and also detoxification of metal ions. Little is known about metal transport into chloroplasts. Until now, the sole chloroplast proteins demonstrated as being involved in metal ions transport are PAA1 (4) and very recently PAA2 (5), two P_{1B}-type ATPases. PAA1, localized into the chloroplast envelope, supplies copper to the chloroplast, whereas PAA2, localized into the thylakoid membrane, delivers copper to the thylakoid lumen. One important result derived from this work is the fact that the disruption of the *PAA1* gene does not fully abolish the import of copper into the chloroplast. From this recent observation, Abdel-Ghany and coworkers (5) concluded that an as yet unidentified and additional way to PAA1 must exist to import copper into the chloroplast.

From proteomic analyses of the *Arabidopsis* chloroplast envelope, we have identified several candidates for metal transport: putative ABC transporters (At1g70610, At2g01320, At5g58270, At5g03910, and At4g25450), a magnesium transporter protein (At5g22830), and the P-type ATPase HMA1 (6).[5]

P-ATPases are transmembrane proteins that couple ATP hydrolysis to the transport of various cations across membranes through a catalytic cycle involving the autophosphorylation of an Asp residue within a highly conserved DKTGT motif. P-ATPases are classified in several subgroups. Transition metal transporters are present within the P_{1B}-ATPase subfamily (7). The vast majority of the characterized P_{1B}-ATPases displays eight predicted transmembrane helices with a typical CPC motif in the sixth helix that is essential for metal transport. They have been classified, respectively, in the P_{1B-1} and P_{1B-2} ATPases subgroup according to their specificity to either Cu^+/Ag^+ or to $Zn^{2+}/Cd^{2+}/Co^{2+}/Pb^{2+}$ (8). Such metal specificities are related to the presence of conserved residues, especially at the level of the seventh and eighth helices and can therefore be predicted from primary sequences. Among the eight P_{1B}-ATPases from *Arabidopsis* (for review see Ref. 9),

* This work was supported by CNRS and CEA (Toxicologie Nucléaire Environnementale) research programs. The costs of publication of this article were defrayed in part by the payment of page charges. This article must therefore be hereby marked "*advertisement*" in accordance with 18 U.S.C. Section 1734 solely to indicate this fact.

[S] The on-line version of this article (available at http://www.jbc.org) contains supplemental Figs. S1–S3

The nucleotide sequence(s) reported in this paper has been submitted to the GenBank™/EBI Data Bank with accession number(s) AY907350.

[1] Both authors contributed equally to this work.
[2] To whom correspondence may be addressed. Tel.: 33-4-3878-4986; Fax: 33-4-3878-5091; E-mail: daphne.berny@cea.fr.
[3] To whom correspondence may be addressed. Tel.: 33-4-3878-4986; Fax: 33-4-3878-5091; E-mail: nrolland@cea.fr.

[4] The abbreviations used are: SOD, superoxide dismutase; Cu/Zn-SOD, Cu/Zn superoxide dismutase; PS, photosystem; ICP-AES, inductively coupled plasma-atomic emission spectrometry; TMs, transmembrane segments; GFP, green fluorescent protein; T-DNA, segment of the Ti plasmid of A. tumifaciens; Ws, Wassilevskija background; MS, Murashige and Skoog.

[5] D. Seigneurin-Berny, J. Joyard, and N. Rolland, unpublished data.

in silico substrate predictions were experimentally confirmed for six transporters: PAA1, PAA2, and RAN1 (members of the P_{1B-1} subgroup) and HMA2, HMA3, and HMA4 (members of the P_{1B-2} subgroup). RAN1 was shown to be involved in the copper intracellular compartmentation allowing the supply of copper to ethylene receptors (10). Concerning HMA2–4, an increasing amount of data supports the predictions that they are involved in zinc, cadmium, and/or lead transport (11–15).

In contrast, the few experimental data on transporters of the P_{1B-4} subgroup, such as HMA1 and OsHMA1, does not allow any accurate substrate and structure predictions. Because disruption of CoaT in *Synechocystis*, an enzyme of this group, reduces Co tolerance and increases Co accumulation (16), it was suggested that proteins of the P_{1B-4} subgroup could be devoted to divalent cation transport, especially cobalt (8).

In this study, we report the identification and functional characterization of a new chloroplast P-type ATPase, HMA1. We first provide evidence for this protein to reside in the chloroplast envelope. We also demonstrate through yeast expression that HMA1 is involved in both zinc and copper homeostasis. Furthermore, characterization of *hma1 Arabidopsis* mutants reveals a decrease in chloroplast copper content and in SOD activity and a photosensitivity phenotype under high light. Finally, measurements of ATPase activity in purified chloroplast envelope membranes demonstrate that HMA1 activity is specifically enhanced by copper. Altogether these results demonstrate that HMA1 is an envelope ATPase involved in delivering copper ions to the stroma, where they are essential for the detoxification of active oxygen species formed during photosynthesis under high light conditions.

EXPERIMENTAL PROCEDURES

Plant Material and Growth Conditions—*Arabidopsis* plants, Wassilevskija background (Ws), were germinated in Petri dishes containing solidified medium (Murashige and Skoog (MS), 1% (w/v) sucrose, and 1% (w/v) agarose) for 2 weeks before transfer to soil. Plants were then grown in culture chambers at 23 °C (12-h light cycle) with a light intensity of 150 μmol·m^{-2}·s^{-1} in standard conditions. For phenotypic analyses, seeds were germinated in plates containing MS salts in the absence or presence of $CuSO_4$ at various concentrations (0.1, 1, 10, and 50 μM), under different light intensities (50, 110, 280, and 340 μmol·m^{-2}·s^{-1}) for 4 weeks.

Purification of Chloroplasts and Chloroplast Subfractions from Arabidopsis—All operations were carried out at 0–5 °C. Percoll-purified chloroplasts were obtained from 100–200 g of *Arabidopsis thaliana* leaves. Crude cell extracts and chloroplast subfractions were purified and stored as previously described (6). Analyses of the purity of chloroplast envelope preparations have shown a contamination with thylakoid protein between 1 and 3% (6). Chloroplasts purified for ICP-AES analyses were washed in the following resuspension buffer: 400 mM sorbitol, 20 mM Hepes/KOH (pH 7.6), 2.5 mM EDTA, 5 mM $MgCl_2$. Protein content was estimated using the Bio-Rad protein assay reagent (17). Chlorophyll content was determined by spectrophotometry in acetone solutions (18).

Isolation of HMA1 Insertional Mutants—The *Arabidopsis hma1* mutants (lines ACT7 and DRC42) were identified by screening the FLAGdb/FST data base (19) from the Institut National de la Recherche Agronomique (Versailles, France) collection of T-DNA insertional mutants. These lines, produced by *Agrobacterium*-mediated transformation (20), were transformed with a T-DNA construct (pGKB5 binary vector) that carries both *bar* and *nptII* selection markers. Primary transformants were self-pollinated to obtain plants homozygous for the insertion. To identify homozygous plants, PCR analyses were carried out on genomic DNA using a primer for the T-DNA (Tag5, CTACAAATTGCCTTTTCTTATCGAC) and a gene-specific primer (FST1, CACCTCGAAGATCAGCCTCG the for ACT7 line and FST2, AGTGAGCTCCTAATGTGCAGAGCTTAAACG for the DRC42 line). In addition, the two gene-specific primers (FST1 and FST2) were used to detect plants that contain only a WT copy of the gene. The amplified bands were sequenced to confirm the T-DNA locations and orientations in *HMA1* gene. Segregation patterns were analyzed by germinating progeny seeds on plates containing MS salts plus kanamycin (100 mg.l^{-1}). Plants selected for further analysis segregated according to a 3:1 ratio, indicative of a single insert.

Construction of Vectors for Stable Expression in Arabidopsis—To construct the vector for HMA1 overexpression in *Arabidopsis* Ws ecotype, the coding region of *HMA1* was PCR-amplified using the two flanking primers BglII-*N*-ter (TCGAGATCTATGGAACCTGCAACTCTTACTC) and SacI-*C*-ter (AGTGAGCTCCTAATGTGCAGAGCTTAAACTG) from an *Arabidopsis* cDNA library. The PCR product was cloned into the pBluescript KS$^-$ vector (Stratagene). The BglII-SacI fragment cleaved from this plasmid was inserted into the BamHI-SacI digested pEL103 binary vector (kanamycin resistance to transform wild-type plants). Plasmids used for *Agrobacterium tumefaciens* transformation were prepared using the "QIAfilter Plasmid Midi Kit" (Qiagen Laboratories; Germany).

Arabidopsis Transformation—Wild-type *Arabidopsis* plants (ecotype Ws) were transformed by dipping the floral buds of 4-week-old plants into an *A. tumefaciens* (C58 strain) solution containing a surfactant (Silwett L-77) according to Clough and Bent (21). Primary transformants were selected on MS medium containing 100 mg·liter^{-1} kanamycin. Only lines segregating 3:1 for the resistance to kanamycin and expressing the recombinant protein were selected for further analysis. Primary transformants were then self-pollinated to obtain plants homozygous for the insertion.

Construction of GFP Reporter Plasmids for Transient Expression in Arabidopsis—The GFP reporter plasmid *Pro35SS:sGFP*(*S65T*) and the plasmid containing the transit peptide (TP) sequence from small unit of Rubisco fused to GFP [*Pro35S:TP-sGFP(S65T)*] were described previously (22). To express HMA1:GFP fusion, we PCR-amplified the entire sequence of *HMA1* using the primers SalI-*N*-ter (TTCGTCGACATGGAACCTGCAACTCTTACTCG) and PciI-*C*-ter (GCAACAGTTTAAGCTCTGCACATCACTGTGG) from an *A. thaliana* cDNA library. The PCR product was cloned into the pBluescript KS$^-$ vector (Stratagene). The SalI-PciI fragment was inserted into the SalI-NcoI-digested GFP reporter plasmid *Pro35SS:sGFP*(*S65T*) to create the *Pro35SS:HMA1-sGFP*(*S65T*) plasmid. From this construct, we extracted the entire cassette Pro35S-HMA1-GFP-Nos Ter using EcoRI and a partial HindIII digestion. This fragment was purified and inserted into the EcoRI-HindIII-digested pEL103 binary vector (kanamycin resistance to transform wild-type plants). The plasmid used for *A. tumefaciens* transformation were prepared using the QIAfilter Plasmid Midi Kit (Qiagen Laboratories).

Arabidopsis Leaves Agroinfiltration—Leaves from *A. thaliana* (ecotype Ws) were injected with *A. tumefaciens* strains harboring the appropriate plasmids according to (23). Three or four days after injection, localization of GFP and GFP fusions in leaves was analyzed by confocal fluorescence microscopy as previously described (24).

Foliar and Chloroplastic Metal Content—Leaves were dried for 48 h at 50 °C. Chloroplasts and dried leaves were mineralized, and metal content was determined using ICP-AES as previously described (25).

RT-PCR—A. thaliana (Ws) plants were grown on sand up to 2 months with an 8-h photoperiod. Total RNA were extracted from various plant tissues with TRIzol (Invitrogen). RT-PCR experiments were performed as previously described (25). We used the following primers to analyze the expression of *HMA1*, *PAA1*, and *PAA2*: HMA1 For (GATCATCACAACCACCATCATC) and HMA1 Rev (CGCTTTTGTATGACAAATCAG); PAA1 For (ACGGGTTATAGCAGGAG) and PAA1 Rev (GTCGTTTCGGTTCGAG); PAA2 For (AAAGGTGGTTTGGCCG) and PAA2 Rev (GGACACTCCCATCGAC); CSD2 For (TCCGTCGAAAGCGTTG) and CSD2 Rev (GCCTCTGACTTAGAGCG).

SDS-PAGE and Western Blot Analyses—SDS-PAGE analyses were performed as described by Chua (26). Proteins were revealed by Coomassie Blue staining. For Western blot analyses, gels were transferred to a nitrocellulose membrane (BA85, Schleicher and Schuell). The polypeptide corresponding to the predicted loop between amino acids 213 and 368 was produced in *Escherichia coli* and purified for the production of a rabbit polyclonal antiserum. This antiserum was used, at a 1/1000 dilution, to detect HMA1. Plasma membrane and mitochondria were purified, from *Arabidopsis*, as previously described (27, 28). To validate purity of the membrane fractions, we used antibodies directed against envelope E37 (29), plasma membrane H^+-ATPase (30), mitochondria TOM40 (31), and thylakoid LHCP (light-harvesting complex proteins) (6).

Superoxide Dismutase Activity—SOD activity was performed according to McCord and Fridovich (32) with the following modifications. The reaction mixture consisted of 50 mM Hepes/KOH (pH 7.8) buffer, 0.5 mM EDTA, 4 mM xanthine, 0.5 mM nitroblue tetrazolium, and 0.01 unit of xanthine oxidase. A concentration curve was produced for each sample to calculate SOD activity. One unit of SOD activity was defined as the amount of extract that inhibited the rate of nitroblue tetrazolium reduction by 50%. The assays were carried out on purified stromal proteins.

Cloning of HMA1—A reverse transcription was performed on poly(A)$^+$ mRNA extracted from leaves of *A. thaliana* (Ws ecotype). The open reading frame of *HMA1* was amplified by PCR using the primers 5′HMA1: CCATGGAACCTGCAACTCTTACTCGTTC and 3′HMA1: CCCCCTAATGTGCAGAGCTTAAACTGTTGC, subcloned in the pCR®-XL-TOPO vector (Invitrogen) and sequenced. This plasmid was modified to insert the NotI restriction site, allowing the subsequent cloning of the full-length cDNA in the pYES2 yeast expression vector (Invitrogen). Two truncated versions of HMA1, HMA1Δ60 and HMA1Δ89, deleted, respectively, from the first 60 and 89 amino acids, were cloned in the pYES2-TOPO vector using, respectively, as forward primers HMA1Δ60for: CCGGAATTCCGGATGCTACGTGCTGTCGAAGATCACCATC and HMA1Δ89for: GGGATGGGATGCTGTTCTGTGGAATTGAAAGCGG. Both reactions were conducted using the reverse primer HMA1rev: AAGGAAAAAAGCGGCCGCAAAAGGAAAACTAATGTGCAGAGCTTAAACTGTTG. Directed mutagenesis was performed on the pYES2-HMA1Δ60 plasmid using the QuikChange® kit (Stratagene), allowing the expression in yeast of D453A, S410C, and H769E substituted versions of HMA1Δ60 or HMA1Δ89.

Yeast Expression, Metal Tolerance, and Accumulation—BY4741 wild-type *Saccharomyces cerevisiae* strain (EUROSCARF acc. no. Y00000) was transformed with the different plasmids and grown on synthetic medium as described in Gravot *et al.* (25), except that the precultures were performed with glucose 2% (w/w) as carbon source to repress the protein expression. Drop-test experiments were performed using $CuSO_4$, $ZnSO_4$, $NiCl_2$, and $CoSO_4$ at various concentrations, and growth was controlled from 2 to 5 days depending on the metal and the concentration. Liquid medium experiments were performed starting from a preculture with 2% (w/w) glucose, diluted in 30 ml to OD = 1 and then cultivated with 2% (w/w) galactose plus 1% (w/w) raffinose for 24 h. Cells were then washed twice with 10 mM EDTA and twice with water. Yeast pellets were then dried at 50 °C and mineralized, and the metal content was analyzed using inductively coupled plasma-atomic emission spectrometer ICP-AES (Vista MPX, Varian).

In Vivo Spectroscopic Estimation of Plastocyanin (PC)/PSI Ratios—Estimation of the PC pool in WT and mutant chloroplasts was performed *in vivo* using an home built spectrophotometer, as previously described (33). Leaves were illuminated by a far red source at 720 nm to oxidize completely the pool of the PSI donors. Alternatively, experiments were performed in the presence of the PSII inhibitor 3-(3′,4′-dichlorophenyl)-1,1-dimethylurea. Absorption changes were detected by discrete flashes provided by a light-emitting-diode source that delivers 10-μs square pulses. Light was filtered with appropriate filters, to select P_{700} and PC redox changes. Absorption changes associated to P_{700} redox changes were computed as ΔI/I 705 nm − ΔI/I 870 nm/2. DI/I PC was computed as ΔI/I 870 nm + ΔI/I 705 nm/10.

ATPase Assay—ATPase activity was measured as the rate of ADP-dependent NADH oxidation in a coupled system containing NADH, phosphoenolpyruvate, pyruvate kinase, and lactate dehydrogenase as described by Blumwald and Poole (34). The activity was monitored in the presence of Mg-ATP and after addition of 3 mM $CuSO_4$, $CoSO_4$, $ZnSO_4$, $FeSO_4$, and $MnSO_4$. The assays were performed on highly purified envelope proteins derived from chloroplasts of WT, *hma1* mutants, and HMA1-overexpressing plants.

Sequence Analyses—Subcellular localizations were predicted using the following programs: ChloroP at www.cbs.dtu.dk/services/ChloroP/ (35) and Predotar at genoplante-info.infobiogen.fr/predotar/ (36). The location of possible transmembrane helices was determined using the program ARAMEMNON at aramemnon.botanik.uni-koeln.de/ (37). Sequence data from this article have been deposited with the GenBank data library under accession number AY907350 for *HMA1* (At4g37270).

RESULTS

HMA1 Is Localized in the Chloroplast Envelope

Primary Sequence Analysis—According to Argüello (8), and as predicted by hydropathy analysis (ARAMEMNON) (37), the membrane topology of HMA1 (At4g37270) suggests the presence of 6 or 7 transmembrane segments (TMs) with 4/5 in the *N*-half of the protein and two downstream of the large loop characterizing P-type ATPases (Fig. 1). HMA1 possesses the typical Ser-Pro-Cys motif in the 4th/5th TM rather than the usual Cys-Pro-Cys/His/Ser motif found in other P_{1B}-ATPases. Furthermore, HMA1 has a His-rich region in its N-terminal part that could play a role in the function or regulation of this transporter, because His residues are often featured in metal-binding domains. The 6 TMs model would put both the His-rich region and the ATPase domain on the same side of the membrane, as for other P_{1B}-ATPases (for review, see Ref. 9). These two domains would then face the intermembrane space of the chloroplast envelope.

In silico analysis using ChloroP on HMA1 primary sequence (35) predicted the presence of a cleavable transit peptide (60 first amino acids; Fig. 1). However, other prediction programs (found in ARAMEMNON) predicted a mitochondrial localization. The experimental validation of the subcellular localization was therefore necessary.

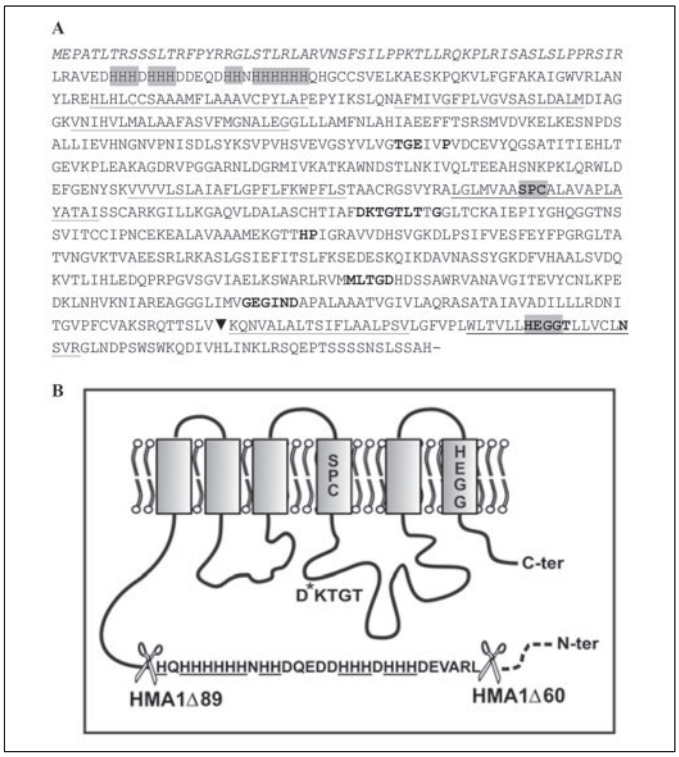

FIGURE 1. **Structure of HMA1.** *A*, primary sequence of HMA1. Predicted transit peptide (from ChloroP (31)) is indicated in *italic*. Transmembrane segments predicted by "ARAMEMNON" and according to Argüello (8) are *underlined*. *Bold* amino acids represent the conserved motifs among the P-type ATPase family. *Gray boxes* indicate the residues that could be involved in metal binding. The *arrow* indicates the position of the T-DNA insertion in mutant lines ACT7 and DRC42. *B*, schematic representation of the structure of HMA1 (adapted from Ref. 8): the *asterisk* indicates the Asp residue, which is phosphorylated during the catalytic cycle. Start codon locations in the H1Δ60 and H1Δ89 versions are indicated by *scissor symbols*.

Validation of the Subplastidial Localization—We first performed transient expression of HMA1-GFP fusion in *Arabidopsis* cells. Because the entire protein fused to GFP was not expressed in this system, we used the 119 first amino acids of HMA1 (including the predicted transit peptide) fused to GFP to transform *Arabidopsis* cells. Consistent with the prediction of ChloroP, HMA1–1/119 fused to GFP was associated to chloroplasts (supplemental Fig. S1). To validate the localization of the full-length protein, we also performed transient expression of HMA1-GFP fusion in *Arabidopsis* leaves. As expected (Fig. 2*A*), GFP alone was localized in the nucleus and the cytoplasm, whereas the plastid control (the transit sequence of the small subunit of Rubisco fused to GFP) was targeted to the chloroplast. HMA1 fused to GFP was only detected in the chloroplasts from both epidermal and parenchymal cells, and no staining was observed in other membranes (Fig. 2*A*).

To strengthen this result, we then performed Western blot experiments on purified subplastidial fractions, purified mitochondria, and plasma membrane proteins. In good agreement with transient expression experiments, HMA1 was only detected in the envelope membranes (Fig. 2*B*) thus excluding the mitochondrial localization predicted in ARAMEMNON database (37). HMA1 was also not detected in two independent plasma membrane preparations thus excluding localization of HMA1 in this membrane system. Finally, the use of antibodies directed against markers from other membrane fractions, clearly demonstrates that association of HMA1 with the chloroplast envelope cannot be due to cross-contamination of envelope preparations with proteins from mitochondria, thylakoids, or plasma membrane.

The expression of *HMA1* was analyzed by RT-PCR. *HMA1* transcripts were mainly detected in green tissues, which is consistent with a

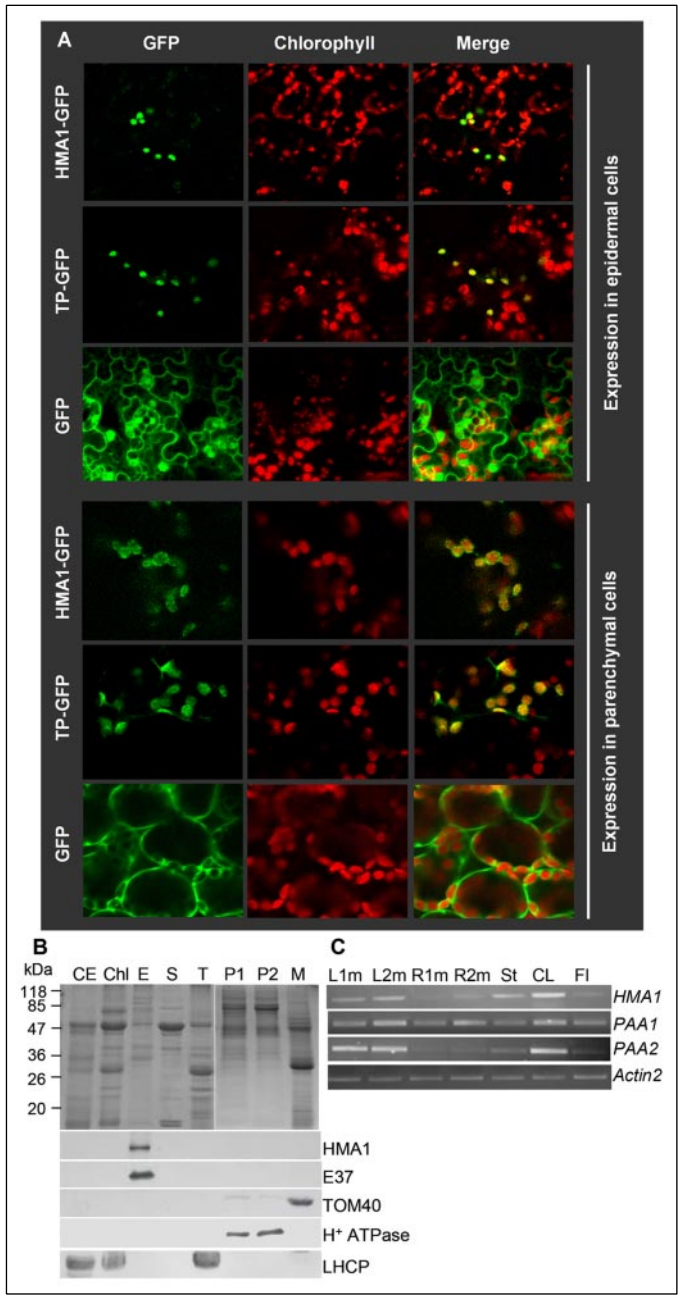

FIGURE 2. **HMA1 is localized in the chloroplast envelope.** *A*, validation of the chloroplast localization by transient expression in *Arabidopsis* leaves. Transit peptide of the small unit of Rubisco fused to GFP (*TP-GFP*) was used as positive control. Localization of the GFP fusion proteins was analyzed in epidermal and parenchymal cells. *B*, Western blots on subplastidial fractions purified as previously described (devoid of any detectable non plastid contamination; see Ref. 6), plasma membrane, and mitochondria. Proteins were analyzed by Coomassie Blue-stained SDS-PAGE (*upper part*) and by Western blot performed with a polyclonal antibody raised against HMA1 (*lower part*). *CE*, crude extract; *Chl*, chloroplasts; *E*, envelope; *S*, stroma; *T*, thylakoids; PM, plasma membrane; and *M*, mitochondria. Each fraction contained 15 μg of proteins. Polyclonal antibodies raised against marker proteins were used to check cross-contaminations of purified fractions (E37 for plastid envelope, TOM40 for mitochondria, H^+ATPase for plasma membrane, LHCP for thylakoids). *C*, expression of *HMA1*, *PAA1*, and *PAA2* transcripts in different tissues. Expression profile was determined by RT-PCR on RNA extracted from various tissues. *ACTIN2* transcript was used as a control. *L1m/L2m*, 1- or 2-month-old rosette leaves; *R1m/R2m*, 1- or 2-month-old roots; *St*, stem; *CL*, cauline leaves; *Fl*, flowers.

chloroplast localization of the protein (Fig. 2*C*). A comparative analysis was performed for the two other previously identified chloroplast Cu-ATPases. A faint expression was observed in roots thus suggesting a possible expression in non-green plastids. In good agreement with the

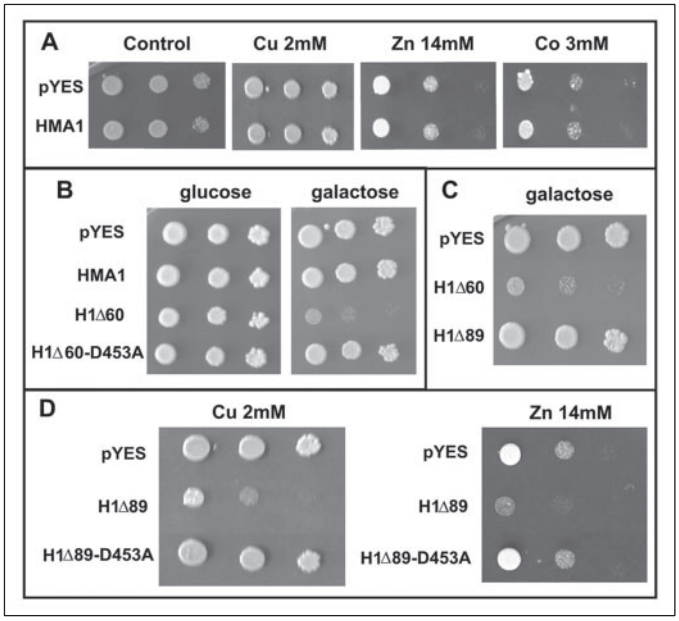

FIGURE 3. **Functional characterization of HMA1 in the yeast system.** Yeast cells with different plasmid (pYES2 as empty control plasmid) were grown as described under "Experimental Procedures," and different dilutions were spotted on plates. *A*, yeast cells expressing the complete cDNA of HMA1 on galactose-containing media supplemented with copper, zinc, or cobalt. *B*, yeast cells expressing HMA1, H1Δ60, and the H1Δ60-D453A substituted version, grown on media inducing (galactose) or repressing (glucose) heterologous protein expression. *C*, yeast cells expressing H1Δ60 and H1Δ89 on galactose containing medium. *D*, yeast cells expressing H1Δ89 and the H1Δ89-D453A substituted version on galactose-containing media supplemented with copper or zinc.

work of Abdel-Ghany *et al.* (5), *PAA2* transcripts were detected in green tissues, whereas *PAA1* transcripts were found in all analyzed tissues (Fig. 2*C*), thus suggesting a broader role of PAA1 in green and non-green plastids.

Functional Characterization of HMA1 by Expression in Yeast

Heterologous Expression of H1Δ60 Impairs Yeast Cell Growth and Leads to Cellular Zinc and Copper Accumulation—Heterologous expression of the complete *HMA1* cDNA was performed in *Saccharomyces cerevisiae* under the control of a galactose-induced promoter. We first observed that the yeast tolerance to zinc, copper, or cobalt was not altered in cells overexpressing HMA1 precursor and grown on metal-containing media (Fig. 3*A*). We also observed that the zinc and cobalt sensitivity of the hypersensitive yeast mutants *zrc1* and *cot1* was not modified by HMA1 overexpression (not shown). To determine whether the lack of phenotype of yeast mutants expressing the full-length HMA1 was due to lack of activity associated with the HMA1 precursor, we expressed in various yeast strains a truncated version of HMA1 (H1Δ60) in which the putative transit peptide (see Fig. 1) was deleted. The growth of H1Δ60-expressing cells was found to be strongly reduced after induction by galactose, even in the absence of excessive metal concentrations (Fig. 3*B*). To determine whether the protein toxicity was linked to its function, we designed a modified version of H1Δ60, in which the phosphorylated Asp-453 from the DKTGT consensus sequence was replaced by an Ala. This substitution is known to prevent the P-ATPase catalytic turnover and impairs metal transport (38). Indeed, when expressed in yeast, the mutated H1Δ60-D453A protein was not toxic (Fig. 3*B*), suggesting that the toxicity of normal H1Δ60 protein could be due to its cation transport capacity. We also analyzed the growth in liquid medium of strains containing either the empty vector, the vector encoding H1Δ60, or the gene encoding the mutated H1Δ60-D453A protein. After an overnight induction with galactose, the optical density of H1Δ60-expressing cells reached only 13% of the optical density found in control cells or in H1Δ60-D453A-expressing cells. Higher levels of copper and zinc were found in H1Δ60-expressing cells compared with control or H1Δ60-D453A-expressing cells (Table 1). As a whole, these results suggest that HMA1 is likely to regulate copper and zinc homeostasis when expressed in yeast cells.

TABLE 1
Metal content in yeast grown on standard medium

Metal content (μg/g DW ± S.D.) in yeast cells expressing the cDNA encoding H1Δ60 or its substituted version H1Δ60-D453A (control with the empty pYES2 plasmid) grown on galactose containing standard medium (metal content of the medium: Cu = 0.236 μM; Zn = 1.5 μM). Values presented represent the average of triplicate measurements ± S.D.

	Zinc	Copper	Manganese
		μg/g DW ± S.D.	
pYES	29.2 ± 3.3	2.24 ± 0.01	1860.6 ± 134.9
HMA1Δ60	186.3 ± 7.2	6.17 ± 0.45	2253.1 ± 68.6
H1Δ60-D453A	34.0 ± 6.9	2.57 ± 0.22	1923.6 ± 143.3

HMA1 His-stretch Deletion Reverses the Yeast Growth Impairment and Reveals a Cu/Zn Hypersensitivity—In many P_{1B}-ATPase, the N-terminal soluble domain is involved in the regulation of metal transport. This is the case for the *CXXC* containing N-terminal HMA domains from Cu^+/Ag^+-ATPases of the P_{1B-1} subgroup. His-rich N-terminal domains of the CopB P_{1B-3}-ATPase from the archaebacterium *Archeoglobus fulgidus* seems to regulate copper transport in a similar way (39), because the deletion of the His-rich N-terminal domain leads to a 40% reduction of the ATPase transport activity, without any modification of the affinity for the transported metal. To investigate the role of the 29-amino acid His-rich stretch downstream the transit peptide (Fig. 1*B*), HMA1 deleted of the first 89 amino acids was expressed in yeast. This H1Δ89 version did not impair the cell growth on standard medium (Fig. 3*C*) suggesting that metal transport activity is affected by the deletion. This allowed testing the sensitivity of the expressing yeast to various metals. H1Δ89-expressing cells were found to be drastically hypersensitive to zinc and copper (Fig. 3*D*) but not to nickel or cobalt (not shown). This phenomenon could reflect a residual metal transport activity of the H1Δ89 truncated protein, which could participate to cell intoxication at very high metal concentration. Indeed, those effects were reversed by the D453A substitution in the DKTGT motif, indicating that metal transport is involved in the observed phenotypes (Fig. 3*D*).

S410C or H769D Substitutions in H1Δ60 Reverse the Lethal Phenotype and Metal Hypersensitivity—Among the numerous specificities shared by the P_{1B-4}-ATPases, are the conserved SPC motif, contrasting with the CPx consensus characteristic of others P_{1B}-ATPases and the conserved HEG(G/S)T in the last predicted helix (8). Site-directed mutagenesis was performed on the pYES2-HMA1Δ60 plasmid to generate the S410C and H769D substitutions, located in the SPC and HEGG motifs from the 4th/5th and the last predicted helix, respectively. We observed that both substitutions reversed the growth impairment phenotype conferred by H1Δ60 expression (Fig. 4). Moreover, neither H1Δ60-S410C nor H1Δ60-H769D expression induced copper or zinc hypersensitivity in the transformed yeast cells. These results suggest that, in contrast with the Δ89 deletion, the S410C and H769D substitutions probably fully abolish metal transport capacities of HMA1. Those two residues are thus likely involved in the metal transduction process rather than in the transport rate regulation.

Functional Characterization of HMA1 by in Planta Analysis

Identification of Homozygous Insertional hma1 Mutants and Production of HMA1-overexpressing Plants—Two T-DNA insertion lines in the *HMA1* gene, lines ACT7 and DRC42 from the FLAGdb/FST data

base (Institut National de la Recherche Agronomique, Versailles, France) were identified. In both lines, the T-DNA is inserted in the 11th intron in the same region but in opposite orientations (Fig. 5*A* and supplemental Fig. S2). We isolated homozygous insertion mutants by segregation analysis on kanamycin and by PCR with specific primers of the *HMA1* gene and with a T-DNA reverse primer (Tag5, corresponding to the 5′ part of the T-DNA; see Fig. 5*A*). Two homozygous mutants were obtained for each insertion line by self-cross, named ACT7 #1, ACT7 #23, DRC42 #4, and DRC42 #12. To analyze the impact of the insertions in these lines, *HMA1* transcripts analyses were performed with various primers in front and behind the T-DNA insertion. In good agreement with the localization of the insertion (Fig. 5*A*), these experiments resulted in the amplification of the 5′ part of *HMA1* mRNA, but no amplification of the 3′ part of *HMA1* could be detected (see Fig. 5*B*). To validate the absence of the HMA1 protein in these lines, subplastidial fractions were prepared from these mutant plants. As shown in Fig. 5*C*, HMA1 was detected in the envelope from WT chloroplasts but not in the envelope from chloroplasts of *hma1* mutants (lines ACT7 and DRC42).

Six stable transformed plants expressing HMA1 under the control of the constitutive ^{35}S promoter were also obtained (see "Experimental Procedures"). For each of these transformants, the amount of HMA1 was determined by Western blot on crude membrane protein extracts. As shown in Fig. 6*A*, HMA1 was detected at a low amount in WT extract, undetected in the extracts from T-DNA insertion lines, and overexpressed in stable transformant plants 1, 2, and 6. We then analyzed by Western blot whether the overexpressed HMA1 was present in envelope membranes. Indeed, it was detected, like the native protein, only in the chloroplast envelope fraction where it was much more abundant (10–20 times) when compared with the native protein detected in WT plants (Fig. 6*B*).

Metal Ion Content in WT, Insertional, and Overexpressing Mutants—When grown in standard conditions, *hma1* and overexpressing mutants did not show any apparent morphological phenotype when compared with WT plants. Because HMA1 is involved in metal transport, we analyzed by ICP the transition metal ions content of these different lines. Leaves and purified chloroplasts were obtained from plants grown in soil in standard conditions. No significant difference was found, in the leaves of these plants, for the content of the various ions analyzed and notably for copper and zinc (Fig. 7*C*). Chloroplast copper levels were comparable in WT and overexpressing plants. However, in chloroplasts from *hma1* mutant lines, copper content was halved with respect to chloroplasts from WT or overexpressing plants (Fig. 7*A*). No difference was observed for the content of chloroplast zinc (Fig. 7*B*), cobalt, or for any other ions analyzed (not shown).

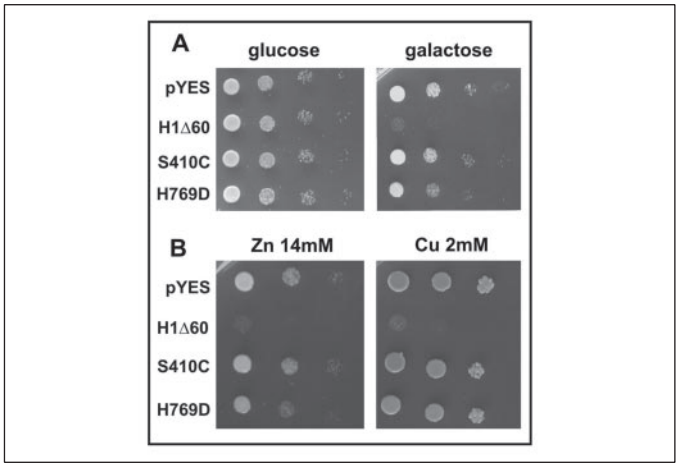

FIGURE 4. **Role of S410 and H769 residues of HMA1.** Yeast cells expressing the cDNA of H1Δ60 and the substituted version H1Δ60-S410C and H1Δ60-H769D were grown on different media. *A*, glucose- or galactose-containing media, respectively, repressing and inducing the yeast heterologous expression. *B*, galactose-containing media supplemented with copper or zinc.

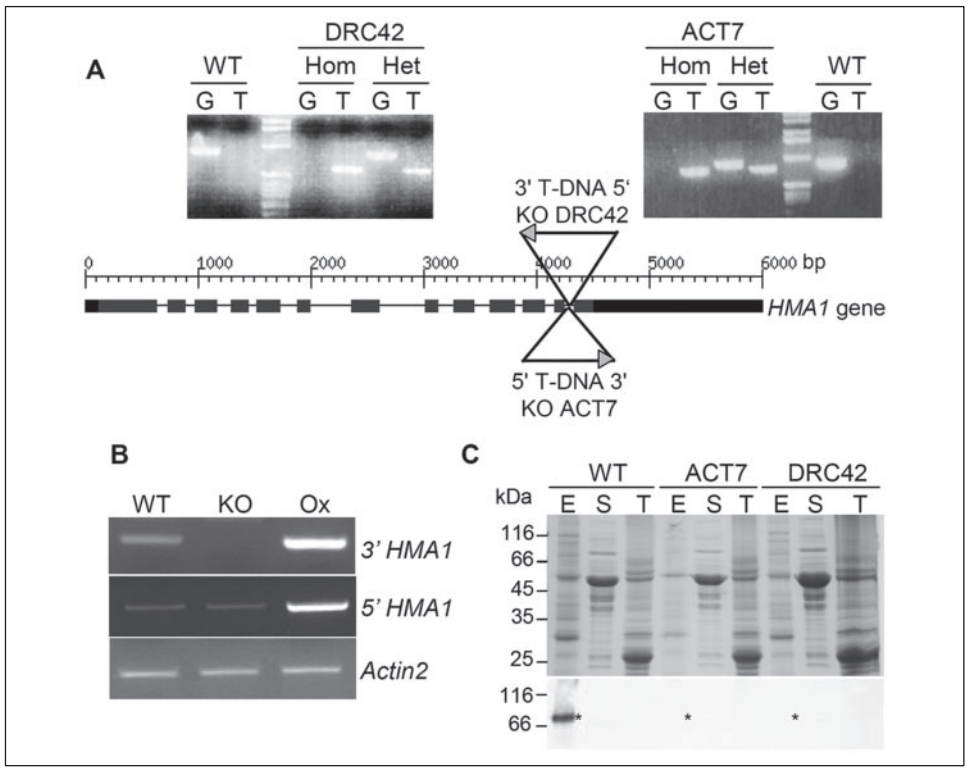

FIGURE 5. **Identification of homozygous *hma1* mutants.** *A*, PCR analyses. The genotype of the two independent insertion lines (ACT7 #1 and DRC42 #12) was analyzed by PCR using a primer for the T-DNA and a gene-specific primer (*T*) or with two gene specific primers (*G*). Both insertions are localized within the 11th intron in opposite orientation. *Hom*, homozygous; *Het*, heterozygous; *WT*, wild type. Similar results were obtained with ACT7 #23 and DRC42 #4 lines (not shown). *B*, expression of *HMA1* in WT plants, *hma1* mutant (KO; ACT7 #23), and HMA1 overexpressing plants (Ox 2). Expression profile of *HMA1* transcripts was determined by RT-PCR on RNA extracted from leaves of the various plants. *ACTIN2* transcript was used as a control. Similar results were obtained with RNA extracted from DRC42 #12 and Ox 1 lines (not shown). *C*, validation of the absence of the HMA1 protein in *hma1* lines. Subplastidial fractions were purified from wild type (*WT*) and mutants (ACT7 #1 and DRC42 #12) plants as previously described (6). Each fraction contained 30 μg of proteins. *E*, envelope; *S*, stroma; *T*, thylakoids. The amount of ACT7 #1 envelope proteins was twice important for the Western blot. Proteins were analyzed by SDS-PAGE and revealed using Coomassie Blue staining, and Western blot with a specific HMA1 antibody. The *stars* indicate the expected positions of HMA1.

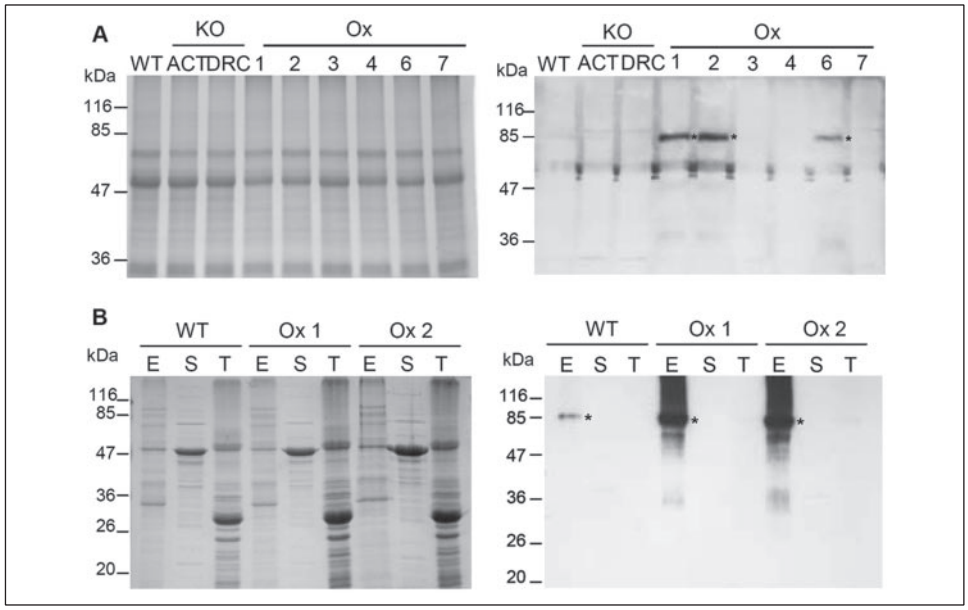

FIGURE 6. **Identification of plants overexpressing HMA1.** *A*, analysis of crude membrane protein extracts from the different genotypes. Membrane proteins were extracted from leaves of WT, KO, and stable transformant plants (*Ox*). Each fraction contained 30 μg of proteins. *KO*, insertion lines ACT7 #1 and DRC42 #12. Six stable transformant lines were obtained by *Agrobacterium* transformation and analyzed for the overexpression of HMA1. *B*, validation of overexpression of HMA1 in the chloroplast envelope. Subplastidial fractions were purified from wild-type (*WT*) and overexpressing plants (*Ox 1* and *2*). Each *lane* contained 15 μg of proteins. *E*, envelope; *S*, stroma; *T*, thylakoids. In *A* and *B*, proteins were analyzed by Coomassie Blue-stained SDS-PAGE and Western blot with an antibody raised against HMA1. The *star* indicates the position of HMA1.

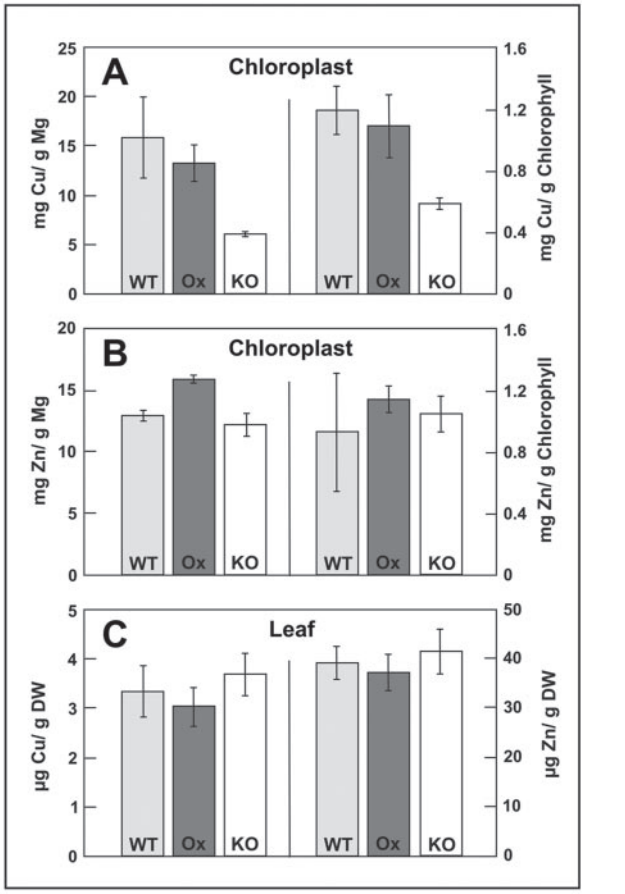

FIGURE 7. **Copper and zinc contents in leaves and chloroplasts purified from WT, *hma1* insertional mutants, and HMA1-overexpressing plants.** Chloroplasts and leaves were mineralized, and the metal content was determined by ICP measurements. Values are normalized according to the amount of magnesium or chlorophyll of the chloroplasts analyzed and according to dry weight for leaves. The values are mean of results obtained from each insertion line (ACT7 #1, #23 and DRC42 #4, #12; *KO*) or overexpressing line (1, 2, and 6; *Ox*). *WT*, wild type. *A*, quantification of copper content in purified chloroplasts. *B*, quantification of zinc content in purified chloroplasts. *C*, Copper and zinc contents in leaves.

Phenotypic Analysis of hma1 Mutants and Overexpressing Plants—Overexpressing and insertional mutant plants did not display any obvious phenotype under standard condition although *hma1* mutants showed a decreased copper content. However, copper is an important cofactor for chloroplast proteins like plastocyanin or SOD (1). We thus tested the impact of copper and of an excess of light on the growth of these different lines. In all conditions tested, the overexpressing plants did not show any visible difference with the WT plants. Under low light intensities (50 and 110 μmol·m^{-2}·s^{-1}, Fig. 8) and for all copper concentrations tested (not shown), we found that *hma1* mutant plants grew like WT plants. In contrast, under high light (above 280 μmol·m^{-2}·s^{-1}), *hma1* mutants exhibited a strong photosensitivity phenotype leading to white leaves with restricted green regions. Some mutant plants were dwarf and totally white, others had several white leaves with some green regions, and a few showed little differences with WT plants. This phenotype was fully reproducible and observed in absence of copper and at various copper concentrations in the media (0.1, 1, and 10 μM). In the presence of 50 μM copper the growth of all plants was affected by the toxic copper concentration and so, differences between WT and *hma1* mutants were less evident. We also noted that this phenotype seems to depend on a threshold, because all the seedlings do not respond similarly and because the leaves show a variegated phenotype. This phenotype demonstrates that HMA1 is necessary to allow plant growth under high light, probably through its role in delivering copper to chloroplast proteins or enzymes highly active in such growth condition.

SOD Activity and Plastocyanin Content—Copper is a cofactor for Cu/Zn-SOD and plastocyanin. We therefore analyzed the SOD activity and the plastocyanin content in chloroplasts of mutants and overexpressing plants. The total SOD activity was measured in stromal proteins purified from all plants. We observed an important diminution of the total SOD activity in the stroma of *hma1* mutant (Fig. 9*B*), whereas no significant difference was observed between stromal SOD activity from WT and overexpressing plants. It is interesting to note that the *CSD2* (the chloroplast Cu/Zn-SOD) transcripts showed a reduced expression in *hma1* mutant leaves (see Fig. 9*A*) when compared with expression levels detected in leaves from WT and overexpressing plants. This is in good agreement with the results of Abdel-Ghany and co-

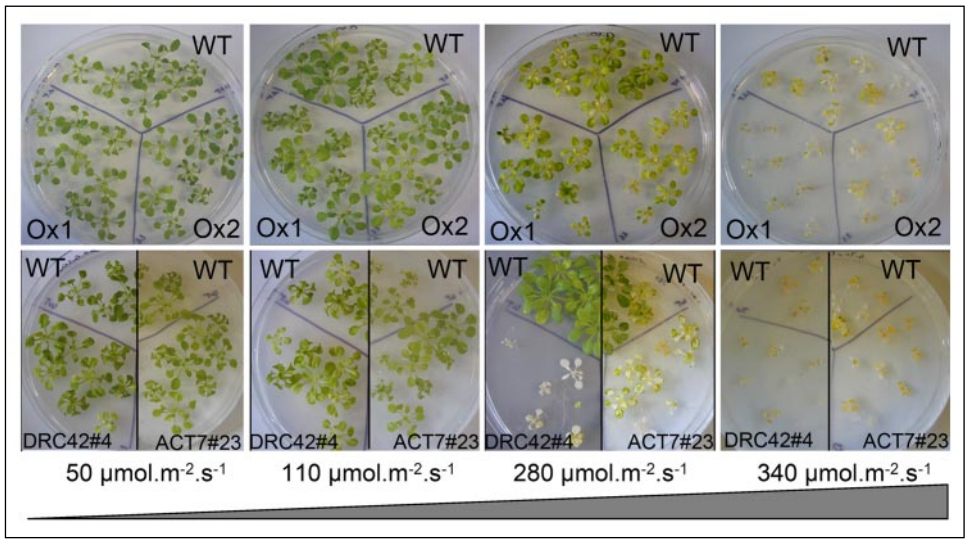

FIGURE 8. **Impact of high light on growth of *hma1* mutants.** Seeds of the different lines were sown on plate containing MS salts and placed in different conditions of light intensity. Growth was monitored during 4 weeks. Insertion lines ACT7 #23 and DRC42 #4 represent one homozygous mutants obtained from the two independent insertion lines ACT7 and DRC42. Other homozygous plants (ACT7 #1 and DRC42 #12) deriving from the same insertion lines presented the same phenotype (not shown). *Ox*: overexpressing plants (*Ox 1* and *2*).

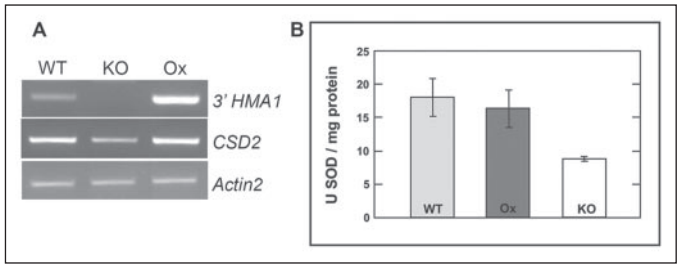

FIGURE 9. **SOD expression and activity.** *A*, expression analysis of *CSD2* transcripts (the chloroplast Cu/Zn-SOD) in leaves from WT, *hma1* mutants (*KO*; ACT7 #23), and HMA1-overexpressing plants (*Ox 2*). Expression profile of *CSD2* and *HMA1* transcripts was determined by RT-PCR on RNA extracted from leaves of the various plants. *ACTIN2* transcript was used as a control. *3′ HMA1*: amplification in the twelve and thirteenth exons, behind insertion of the T-DNA. *B*, measurement of the total SOD activity (Cu/Zn and iron SODs) in purified chloroplasts from WT, *hma1* mutants, and HMA1-overexpressing plants. SOD activity was measured spectrophotometrically on stromal proteins. *WT*, wild type; *KO*, mean value obtained for the four insertional lines (ACT7 #1, #23 and DRC42 #4, #12); *Ox*: mean value obtained for the three overexpressing line (*Ox 1*, *2*, and *6*).

workers (5) who showed that the decrease of copper in the stroma leads to a decrease of the CSD2 activity (resulting from the lack of copper) but also to a decrease of the *CSD2* transcripts. They have suggested that copper is sensed in the stroma of the chloroplast and that this signal influences transcript level of the chloroplast Cu/Zn-SOD (5).

We then analyzed the plastocyanin content of mutant and WT chloroplasts by spectroscopic analysis *in vivo*. In contrast to SOD, the plastocyanin levels were not affected in the lumen of *hma1* mutant chloroplasts (Table 2). This suggests that either the affinity of the plastocyanin for copper is enough to compensate for a decrease in copper chloroplast concentration induced by the mutation, or that the affinity of the thylakoidal copper-transport machinery is large enough to maintain copper homeostasis in the thylakoid lumen.

ATPase Assay on Chloroplast Envelope—To have a direct biochemical evidence for the ATPase activity and specificity of the HMA1 protein, we choose to measure its activity on chloroplast envelope membranes purified from the different plants available. This assay was performed to determine (*a*) whether the expression level of HMA1 could modify the ATPase activity of the chloroplast envelope and (*b*) whether this activity was modified by the presence of ions. This assay allows the measurement of total envelope ATPase activities, including PAA1, HMA1 (two P_{1B}-type ATPases, which may be sensitive to addition of metal ions), and other unidentified ATPases of the chloroplast envelope.

TABLE 2
PC/PSI stoichiometry in WT and mutant leaves

Values refer to the size of the PC pool, normalized to the amount of $P700^+$. They represent the average of quadruplicate measurements performed on WT and two independent mutant lines ACT7 #23, DRC42 #12 and Ox 1, Ox 2 ± S.D. Similar results were obtained when the inhibitor DCMU was added to fully block photosystem II activity (not shown).

Strain	WT	*hma1* mutants	Overexpressing plants
PC/PSI ratio	3 ± 0.40	2.9 ± 0.45	3.1 ± 0.38

As shown in Table 3, the ATPase activity associated to chloroplast envelope membranes is reduced in *hma1* mutants (*hma1* KO) due to the lack of HMA1 activity. On the contrary, this ATPase activity is enhanced in envelope membranes from plants overexpressing the HMA1 protein (Ox 1, -2, and -6; see Fig. 6). This first observation is in good agreement with an ATPase activity associated to the HMA1 protein.

It is important to note that ATPase activities of very similar values were measured in the presence of cobalt or zinc ions (Table 3) suggesting that these ions have no impact on the HMA1 activity (but also on any other chloroplast envelope associated ATPases). Similarly, addition of silver, manganese, or iron did not affect the ATPase activity measured in the envelope from the various plants (not shown). However, when the assay was performed in the presence of copper, a significant increase of the ATPase activity was detected, especially in the envelope from HMA1 overexpressing plants (Ox; see Table 3). This second observation clearly demonstrates that HMA1 activity is specifically stimulated by copper. The increase of the total ATPase activity observed in the envelope from the *hma1* insertion mutants and in the presence of copper is most probably due to the activation of the PAA1 protein, because this ATPase was also demonstrated to be associated to the chloroplast envelope and involved in copper homeostasis (see Ref. 5). This experiment then provides the first direct biochemical evidence for a copper-stimulated ATPase activity associated to both HMA1 and PAA1. The increase of total ATPase activity observed in envelope from WT plants then most probably accounts for the stimulation of both HMA1 and PAA1.

To have an estimation of the respective activities of HMA1 and PAA1 (and other yet uncharacterized chloroplast envelope ATPases), we compared the ATPase activities measured in the envelope from WT, *hma1* mutants, and overexpressing plants. This provides an estimate of (*a*) the

TABLE 3

HMA1 ATPase activity in envelope membranes is specifically enhanced by copper

The total ATPase activity was measured in chloroplast envelope membranes purified from WT plants, the two independent *hma1* mutants (KO) and the three HMA1 overexpressing plants (Ox). WT: mean value ± S.D. obtained for the two independent envelope preparations from WT plants. *hma1* KO: mean value ± S.D. obtained for the two independent insertional lines (ACT7 #23 and DRC42 #12); Ox: mean value ± S.D. obtained for the three independent HMA1 overexpressing lines (Ox 1, 2, and 6). The comparison of the activities obtained from the different genotypes gives access to an estimation of (*a*) the specific activity of HMA1 and (*b*) PAA1 and other potential ATPases activity (activity measured in *hma1* mutants). The sum of S.D. obtained for biochemical assays was added to estimated values of HMA1 activity (activity in WT or Ox lines minus activity in *hma1* mutant). 100% correspond to the value of ATPase activity measured in WT envelope in the presence of Mg-ATP, *i.e.* 0.46 ± 0.003 μmol/h/mg envelope proteins.

	Genotype lines	Mg-ATP	Mg-ATP plus cobalt	Mg-ATP plus zinc	Mg-ATP plus copper
Measured ATPase activity (%) as measured on highly puridied chloroplast envelope fractions	WT	100 ± 0.7	103 ± 1.3	103 ± 1.8	260 ± 1.1
	*hma1*KO	63 ± 8	66 ± 6	79 ± 12	204 ± 5
	Ox	170 ± 24	185 ± 20	175 ± 25	641 ± 20
Estimation of PAA1 (and other ATPases) activity (%) as deduced from the specific activity measured in *hmal* mutants	WT	63 ± 8	66 ± 6	79 ± 12	204 ± 5
	*hma1*KO	63 ± 8	66 ± 6	79 ± 12	204 ± 5
	Ox	63 ± 8	66 ± 6	79 ± 12	204 ± 5
Estimation of HMA1 ATPase (%) as deduced from the total ATPase activity minus PAA1 and other ATPase activity	WT	37 ± 8.7	37 ± 7.3	24 ± 13.8	56 ± 6.1
	*hma1*KO	0	0	0	0
	Ox	107 ± 30	119 ± 26	96 ± 37	437 ± 25

specific activity of HMA1 and (*b*) the PAA1 and other ATPase activity. Indeed, the activity measured in the envelope from *hma1* mutants corresponds to the PAA1 activity and other unidentified ATPases of the chloroplast envelope. Thus, subtraction of the total activity measured in WT or overexpressing plant to the activity measured in the *hma1* mutant gives an estimation of the specific activity of HMA1 in these plants (see Table 3).

On this basis, one can note that the HMA1 activity is increased about 12 times in overexpressing plant and in the presence of copper (Table 3), which is in good agreement with the level of accumulation of overexpressed HMA1 protein in envelope membrane from these plants (see Fig. 6).

Finally, and in good agreement with these direct biochemical observations, we could demonstrate that deletion or overexpression of HMA1 has no impact on the expression of both PAA1 and PAA2 (supplemental Fig. S3). Both biochemical analysis and expression studies (Table 3 and supplemental Fig. S3) thus demonstrate that PAA1 cannot compensate for the lack of HMA1.

DISCUSSION

HMA1 Is a P_{1B}-ATPase of the Chloroplast Envelope—Proteomic analyses of chloroplast envelope membranes (Refs. 6, 40, and unpublished results) led to the identification of hundreds of proteins, among which we found HMA1 that belongs to the P_{1B}-ATPases, a subgroup of the P-type ATPases involved in metal ions transport (3). We demonstrated its chloroplast envelope localization using both transient expression in *Arabidopsis* leaves and cultured cells and Western blot analyses performed on subplastidial fractions (Fig. 2). HMA1 is therefore the second P_{1B}-ATPase identified in the chloroplast envelope, the first one being the ATPase PAA1 (5). The presence of such transporters was expected, because metals play a key role in chloroplast metabolism. HMA1 belongs to the P_{1B-4}-ATPases, which display only 6 (8) or 7 (ARAMEMNON) predicted helix instead of 8 and share a specific SPC motif instead of the classical CPx consensus. HMA1 lacks the N-terminal *Heavy Metal Associated* regulatory domain usually found in P_{1B}-ATPases. Instead, it has a long His stretch reminding the N-terminal domain of the P_{1B-2} Bxa1 from *Oscillatoria brevis* that was described as transporting both copper and zinc (41).

It is worthy to note that the orthologue OsHMA1 in rice shares the same structural properties (42) and is predicted to be chloroplast located by Predotar (36). Moreover the green alga *Chlamydomonas reinhardtii* displays two putative organelle-targeted P_{1B}-ATPases, namely CrHMA1 and CrHMA3, that are respectively orthologues of HMA1 and PAA1/PAA2 (43), suggesting that the presence of two subgroups of copper transporting P_{1B}-ATPases is necessary even in this phylogenetically distant photosynthetic eukaryote. In *Cyanidioschizon merolae*, a unicellular red alga considered to belong to the most primitive eukaryotic phylum (44), CmHMA1 is even the only putative organelle-targeted P_{1B}-ATPase (43). This suggests an essential role for this transporter in supplying copper to the single chloroplast of this organism.

HMA1 Expression in Yeast Affects Copper and Zinc Homeostasis—Yeast heterologous expression is an efficient tool that allowed the functional characterization of many plant metal transporters. The fact that yeast cells expressing H1Δ60 contain more copper and zinc than wild type cells reflects an impairment of the homeostasis for those two metals. A possibility would be that H1Δ60 is addressed to the yeast plasma membrane, importing copper and zinc from the medium into the cytoplasm. The major drawback of this hypothesis is that P_{1B}-ATPases are generally considered to transport metals from the cytoplasmic side of membranes to the other side (8). A more likely hypothesis is that H1Δ60 is addressed to yeast internal membranes, loading copper and zinc from the cytoplasm into a metal-sensitive compartment. The resulting cytoplasmic metal depletion could trigger an enhancement of metal import processes, accounting for the higher copper and zinc content in H1Δ60-expressing cells.

Because H1Δ60-expressing cells grow at a very low rate, we were unable to test whether added metals could accentuate the lethal phenotype to validate that metal homeostasis impairment is the actual cause of the growth stop. In H1Δ89-expressing cells, a residual transport activity offers the possibility to explore metal specificity of HMA1. The fact, that such yeast cells were still highly sensitive to copper and zinc, suggests that both metals can be transported by HMA1 in yeast. However, due to the copper specificity of HMA1 observed *in planta* (low copper content in the chloroplasts from *hma1* knock-out lines and copper-specific stimulation of HMA1 activity, see latter) we cannot exclude that the impact of HMA1 expression on zinc concentrations measured in yeast cells results from an indirect effect.

Proteins from the P_{1B-4}-subgroup display strong originality at the structural level, the first being the number of predicted helices, which is probably lower than the 8 helices found in P_{1B-1}- and P_{1B-2}-ATPases. Both OsHMA1 and HMA1 display a His-rich motif at the N-terminal part of the protein. Yeast expression experiments (Fig. 3) led to the conclusion that this stretch could play a role in metal transport regula-

tion. This is consistent with experiments performed on His-rich domains in other P_{1B-3}-ATPases (39) and P_{1B-2}-ATPases (15).

The CPx motif in the 6th predicted helix is widely accepted as a component of a metal translocation/binding site. However, a recent study with CopA from *Archaeoglobus fulgidus* demonstrated that other residues from the 7th and the 8th helices are required for Cu^+ coordination during transport (45). The present study strongly suggests that the Ser residue from the SPC motif in HMA1 is essential for metal transport and that it cannot be substituted by a Cys. We also showed that the His residue from the HEGG motif in the last helix probably plays a role in transport. This confirms the alignment-based predictions of Argüello (8) and highlights the specificity of the Ser residue in P_{1B-4}-ATPases.

Disruption of HMA1 Affects Copper Content in Chloroplasts and Leads to Photosensitivity under High Light Conditions—Whereas the metal content in leaves from the different genotypes was comparable, the copper content in *hma1* mutant chloroplasts was only half the one in WT plants (Fig. 7). This result points out the importance of analyzing purified chloroplasts as the copper deficiency was undetectable at the organ level. Altogether, the data from yeast expression and the low copper content in *hma1* chloroplasts suggest that HMA1 is involved in copper uptake into chloroplasts. The specificity of HMA1 for copper was also confirmed by direct biochemical evidences, because ATPase assays performed on chloroplast envelope demonstrated that HMA1 ATPase activity was exclusively stimulated by copper and not by zinc, cobalt, iron, manganese, or silver. As the specificity of the protein deduced from its expression in heterologous system is slightly different to the one identified in its native context, this underlined the importance of the characterization *in planta*. This specificity for copper is in perfect correlation with the reduced content of copper ions measured in chloroplasts from *hma1* plants. The resulting copper content in *hma1* chloroplasts is likely to result from PAA1 activity (5) or other still unidentified copper transporters.

In chloroplasts, copper is a cofactor for plastocyanin that transfers electrons from cytochrome b_6f to PSI and for the chloroplast Cu/Zn-SOD that is a critical component of the active-oxygen-scavenging system (46). Thus, we analyzed the impact of copper and high light on the growth of the mutant lines. High concentration of copper (50 μM) led to the inhibition of leaf expansion and destruction of chlorophylls. This toxicity appeared for all the plants analyzed (data not shown) probably due to a toxic cytoplasm copper concentration. Surprisingly, there was no phenotypic variation between WT, overexpressing, and insertional plants for all copper concentrations used. No enhanced sensitivity of overexpressing plants to copper was observed, which is consistent with the WT levels of copper found in the chloroplasts from overexpressing plants. This suggests a tight regulation of the cell copper uptake and also the presence of a copper regulation system in the chloroplast such as saturation of metallochaperone or presence of protein involved in copper efflux.

Under high light, the *hma1* lines present a photobleaching that is not observed in WT and overexpressing plants (Fig. 8). This photosensitivity was not rescued by addition of copper in the medium. Such a phenotype is consistent with the diminution of the copper content in chloroplasts from *hma1* mutants. Cu/Zn-SODs are ubiquitous metalloenzymes that catalyze the reduction of superoxide (O_2^-) to hydrogen peroxide and molecular oxygen (32), a reaction that constitutes the first cellular defense against many oxidative stress situations (47). Reactive oxygen species, like O_2^-, are mainly formed in the chloroplast where light harvesting and electron transport lead to the formation of singlet oxygen and superoxide anion radicals (48). In this study, in *hma1* mutant grown in normal conditions, we found a reduction of the total chloroplast SOD activity but no variation of the plastocyanin content (Fig. 9 and Table 2). The diminution of SOD activities could account for the photosensitivity phenotype. Different pathways are thought to cooperate to respond to photooxidative stress: the zeaxanthin cycle, the cyclic electron flow, and the water-water cycle that involve SOD and ascorbate peroxidase enzymes (49). Characterization of chloroplast Cu/Zn-SOD knockdown and overexpressing plants suggest that this SOD plays an essential role in photooxidative stress (46, 49).

We can hypothesize that under low light intensity, the remaining level of copper in chloroplasts from *hma1* mutant plants is sufficient to supply the needs for the active plastocyanin and part of the chloroplast SOD. In these conditions, the remaining SOD activity is sufficient to scavenge the low amount of reactive oxygen species that are produced. However, under higher light intensity, the release of reactive oxygen species is enhanced and SODs have to respond to this oxidative stress. In this case, chloroplast SOD activities in the *hma1* mutant are probably insufficient to reduce the pool of reactive intermediates produced, causing destruction of chlorophylls and, in turn, inhibition of photosynthesis. This observation also suggests that other photoprotection systems are not able to compensate for the decrease of SOD activity.

Which Function for HMA1 in the Chloroplast?—HMA1 and PAA1 are two P_{1B}-type ATPases involved in the transport of copper into chloroplasts, but the disruption of the corresponding genes have different consequences. *hma1* mutants contain less chloroplast copper and SOD activity without any detectable impact on plastocyanin and pigment contents. *hma1* mutants also display a photosensitivity phenotype under high light, that is not reversed by addition of copper in the media. In *paa1* mutants (4), copper content is also halved, but the pool of plastocyanin is severely affected and the activity of Cu/Zn-SOD, electron transport, and chlorophyll content are diminished. Furthermore, copper addition rescues the *paa1* phenotype. Altogether, these results suggest that these two P_{1B}-ATPases play different roles in the regulation of copper homeostasis and transport.

From our observations and the data from Abdel-Ghany *et al.* (5), we can conclude that the *Arabidopsis hma1* and *paa1* mutants have a different behavior upon addition of copper to the culture medium. *paa1* mutants recover a WT phenotype (5) probably owing to the action of the HMA1 protein and its capacity to import copper. In contrast, in *hma1* mutants, the phenotype observed is not reversed by addition of copper, thus PAA1 seems to function at its maximum rate and is probably not able to provide more copper to the chloroplast. This hypothesis is reinforced by ATPase measurements (Table 3), which showed, in *hma1* mutant and in the presence of high concentration of copper (3 mM), that PAA1 is unable to compensate for the lack of HMA1 activity.

P_{1B}-ATPases are generally specific to either monovalent or divalent cations. Because copper can be found both as a monovalent or divalent ion, the apparent redundancy between HMA1 and the recently described P_{1B-1}-ATPase PAA1 at the chloroplast envelope could hide their specific role in the transport of divalent and monovalent copper. Further biochemical work is needed to ascertain this hypothesis.

It has been proposed that PAA1 provides copper to a metallochaperone that could interact with the chloroplast Cu/Zn-SOD and also to PAA2, a P_{1B}-ATPase localized in the thylakoids (5). Then, PAA1 could be the major copper transport system into chloroplasts to supply copper for photosynthesis. This hypothesis is strengthened by our measurements of ATPase activities in purified envelope membranes from overexpressing plants. These assays show that HMA1 activity represents about one-third of the total activity (see Table 3) in the various conditions analyzed. As it seems unlikely that other Cu-ATPases are present

in the chloroplast envelope, the increase of activity observed in the presence of copper is most likely due to HMA1 and PAA1 activities. Thus, by comparing the results obtained in control condition and in the presence of copper for WT and *hma1* mutant lines (Table 3), we estimated that HMA1 activity increases 1.5 times (from 37% to 56% with copper) and PAA1 activity at least 3.2 times (from 63% to 204% with copper, and considering that the 63% can account for other ATPase activity). On a quantitative point of view, the activity of HMA1 seems thus to be lower than that of PAA1 in the chloroplast envelope. However, it should be kept in mind that, despite its lesser ATPase activity levels, HMA1 physiological function seems to be irreplaceable in light-stressing conditions as *PAA1* gene expression and PAA1 protein activity cannot compensate for the lack of HMA1.

Although more expressed in leaves when compared with non-green tissues, PAA1 is relatively abundant in all tested plant tissues (Fig. 2*C*). On the contrary, HMA1 is mainly expressed in green tissues suggesting that it is important for an optimal functioning of chloroplasts. Interestingly, HMA1 and PAA2 present very similar expression profiles (Fig. 2*C*) thus suggesting that the role of both enzymes is more important in chloroplasts where larger amounts of copper might be required for photosynthesis (PAA2) and to respond to oxidative stress (HMA1). A weak expression of HMA1 was also detected in roots. This might be related to the fact that a Cu/Zn-SOD seems to be present in plastids of roots (50, 51) and that oxidative stresses also occur in roots. We thus cannot exclude a role for HMA1 in non-green plastids.

Finally, our work suggests that plastids need different copper transport systems and a tight regulation of these copper delivering pathways to supply photosynthesis and to respond to oxidative stress generated in high light conditions. PAA1 and HMA1 are not just redundant proteins in term of physiological function. Then, more than identifying an alternative import pathway for copper, we provide evidence for an alternative role of HMA1, which is its specific requirement for the plant to grow under adverse light conditions.

Acknowledgments—We thank Marinus Pilon for sending proofs of his manuscript before publication. We also thank Ariane Atteia for critical reading of the manuscript, Geneviève Ephritikhine for the purified plasma membrane proteins, and Solène Kowalski for the purified mitochondria. The TOM40, H^+-ATPase, and LHCP antibodies were obtained from Wolf Werhahn, Marc Boutry, and Olivier Vallon, respectively. Maryse Block is acknowledged for the gift of the E37 antibody. Thierry Lagrange is acknowledged for providing the pEL103 binary vector (originally constructed by Eric Lam).

REFERENCES

1. Fox, T. C., and Guerinot, M. L. (1998) *Plant Mol. Biol.* **49,** 669–696
2. Raven, J. A., Evans, M. C. W., and Korb, R. E. (1999) *Photosynth. Res.* **60,** 111–149
3. Williams, L. E., Pittman, J. K., and Hall, J. L. (2000) *Biochim. Biophys. Acta* **1465,** 104–126
4. Shikanai, T., Müller-Moulé, P., Munekage, Y., Niyogi, K. K., and Pilon, M. (2003) *Plant Cell* **15,** 1333–1346
5. Abdel-Ghany, S. E., Müller-Moulé, P., Niyogi, K. K., Pilon, M., and Shikanai, T. (2005) *Plant Cell* **17,** 1–19
6. Ferro, M., Salvi, D., Brugiere, S., Miras, S., Kowalski, S., Louwagie, M., Garin, J., Joyard, J., and Rolland, N. (2003) *Mol. Cell. Proteomics* **2,** 325–345
7. Palmgren, M. G., and Axelsen, K. B. (1998) *Biochim. Biophys. Acta* **1365,** 37–45
8. Argüello, J. M. (2003) *J. Membr. Biol.* **195,** 93–108
9. Williams, L. E., and Mills, R. F. (2005) *Trends Plant Sci.* **10,** 491–502
10. Hirayama, T., Kieber, J. J., Hirayama, N., Kogan, M., Guzman, P., Nourizadeh, S., Alonso, J. M., Dailey, W. P., Dancis, A., and Ecker, J. R. (1999) *Cell* **97,** 383–393
11. Mills, R. F., Krijger, G. C., Baccarini, P. J., Hall, J. L., and Williams, L. E. (2003) *Plant J.* **35,** 164–176
12. Mills, R. F., Francini, A., Ferreira da Rocha, P. S., Baccarini, P. J., Aylett, M., Krijger, G. C., and Williams, L. E. (2005) *FEBS Lett.* **579,** 783–791
13. Hussain, D., Haydon, M. J., Wang, Y., Wong, E., Sherson, S. M., Young, J., Camakaris, J., Harper, J. F., and Cobbett, C. S. (2004) *Plant Cell* **16,** 1327–1339
14. Verret, F., Gravot, A., Auroy, P., Leonhardt, N., David, P., Nussaume, L., Vavasseur, A., and Richaud, P. (2004) *FEBS Lett.* **576,** 306–312
15. Verret, F., Gravot, A., Auroy, P., Preveral, S., Forestier, C., Vavasseur, A., and Richaud, P. (2005) *FEBS Lett.* **579,** 1515–1522
16. Rutherford, J. C., Cavet, J. S., and Robinson, N. J. (1999) *J. Biol. Chem.* **274,** 25827–25832
17. Bradford, M. (1976) *Anal. Biochem.* **72,** 248–254
18. Bruinsma, J. (1961) *Biochim. Biophys. Acta* **52,** 576–578
19. Samson, F., Brunaud, V., Balzergue, S., Dubreucq, B., Lepiniec, L., Pelletier, G., Caboche, M., and Lecharny, A. (2002) *Nucleic Acids Res.* **30,** 94–97
20. Bechtold, N., Ellis, J., and Pelletier, G. (1993) *CR Acad. Sci. Paris Life Sci.* **316,** 1194–1199
21. Clough, S. J., and Bent, A. F. (1998) *Plant J.* **16,** 735–743
22. Chiu, W., Niwa, Y., Zeng, W., Hirano, T., Kobayashi, H., and Sheen, J. (1996) *Curr. Biol.* **6,** 325–330
23. Lavy, M., Bracha-Drori, K., Sternberg, H., and Yalovsky, S. A. (2002) *Plant Cell* **14,** 2431–2450
24. Miras, S., Salvi, D., Ferro, M., Grunwald, D., Garin, J., Joyard, J., and Rolland, N. (2002) *J. Biol. Chem.* **277,** 47770–47778
25. Gravot, A., Lieutaud, A., Verret, F., Auroy, P., Vavasseur, A., and Richaud, P. (2004) *FEBS Lett.* **561,** 22–28
26. Chua, N. H. (1980) *Methods Enzymol.* **69,** 434–436
27. Marmagne, A., Rouet, M. A., Ferro, M., Rolland, N., Alcon, C., Joyard, J., Garin, J., Barbier-Brygoo, H., and Ephritikhine, G. (2004) *Mol. Cell. Proteomics* **3,** 675–691
28. Brugiere, S., Kowalski, S., Ferro, M., Seigneurin-Berny, D., Miras, S., Salvi, D., Ravanel, S., d'Herin, P., Garin, J., Bourguignon, J., Joyard, J., and Rolland, N. (2004) *Phytochemistry* **65,** 1693–1707
29. Teyssier, E., Block, M. A., Douce, R., and Joyard, J. (1996) *Plant J.* **10,** 903–912
30. Morsomme, P., Dambly, S., Maudoux, O., and Boutry, M. (1998) *J. Biol. Chem.* **273,** 34837–34842
31. Werhahn, W., Niemeyer, A., Jansch, L., Kruft, V., Schmitz, U. K., and Braun, H. (2001) *Plant Physiol.* **125,** 943–954
32. McCord, J. M., and Fridovich, I. (1969) *J. Biol. Chem.* **244,** 6049–6055
33. Joliot, P., and Joliot, A. (2005) *Proc. Natl. Acad. Sci. U. S. A.* **102,** 4913–4918
34. Blumwald, E., and Poole, R. J. (1985) *Proc. Natl. Acad. Sci. U. S. A.* **82,** 3683–3687
35. Emanuelsson, O., Nielsen, H., and von Heijne, G. (1999) *Protein Sci.* **8,** 978–984
36. Small, I., Peeters, N., Legeai, F., and Lurin, C. (2004) *Proteomics* **4,** 1581–1590
37. Schwacke, R., Schneider, A., Van Der Graaff, E., Fischer, K., Catoni, E., Desimone, M., Frommer, W. B., Flügge, U. I., and Kunze, R. (2003) *Plant Physiol.* **131,** 16–26
38. Møller, J. V., Juul, B., and le Maire, M. (1996) *Biochim. Biophys. Acta* **1286,** 1–51
39. Mana-Capelli, S., Mandal, A. K., and Argüello, J. M. (2003) *J. Biol. Chem.* **278,** 40534–40541
40. Ferro, M., Salvi, D., Rivière-Rolland, H., Vermat, T., Seigneurin-Berny, D., Garin, J., Joyard, J., and Rolland, N. (2002) *Proc. Natl. Acad. Sci. U. S. A.* **99,** 11487–11492
41. Tong, L., Nakashima, S., Shibasaka, M., Katsuhara, M., and Kasamo, K. (2002) *J. Bacteriol.* **184,** 5027–5035
42. Baxter, I., Tchieu, J., Sussman, M. R., Boutry, M., Palmgren, M. G., Gribskov, M., Harper, J. F., and Axelsen, K. B. (2003) *Plant Physiol.* **132,** 618–628
43. Hanikenne, M., Krämer, U., Demoulin, V., and Baurain, D. (2005) *Plant Physiol.* **137,** 428–446
44. Matsuzaki, M., Misumi, O., Shin, I. T., Maruyama, S., Takahara, M., Miyagishima, S. Y., Mori, T., Nishida, K., Yagisawa, F., Nishida, K., Yoshida, Y., Nishimura, Y., Nakao, S., Kobayashi, T., Momoyama, Y., Higashiyama, T., Minoda, A., Sano, M., Nomoto, H., Oishi, K., Hayashi, H., Ohta, F., Nishizaka, S., Haga, S., Miura, S., Morishita, T., Kabeya, Y., Terasawa, K., Suzuki, Y., Ishii, Y., Asakawa, S., Takano, H., Ohta, N., Kuroiwa, H., Tanaka, K., Shimizu, N., Sugano, S., Sato, N., Nozaki, H., Ogasawara, N., Kohara, Y., and Kuroiwa, T. (2004) *Nature* **428,** 653–657
45. Mandal, A. K., Yang, Y., Kertesz, T. M., and Argüello, J. M. (2004) *J. Biol. Chem.* **279,** 54802–54807
46. Gupta, A. S., Webb, R. P., Holaday, A. S., and Allen, R. D. (1993) *Plant Physiol.* **103,** 1067–1073
47. Bowler, C., Van Camp, W., Van Montagu, M., and Inzé, D. (1994) *CRC Crit. Rev. Plant Sci.* **13,** 199–218
48. Levine, A. (1999) in: *Plant Responses to Environmental Stresses* (Lerner, H. R., ed) pp. 247–264, New York, Marcel Dekker Inc
49. Rizhsky, L., Liang, H., and Mittler, R. (2003) *J. Biol. Chem.* **278,** 38921–38925
50. Kliebenstein, D. J., Monde, R. A., and Last, R. L. (1998) *Plant Physiol.* **118,** 637–650
51. Ruzsa, S. M., and Scandalios, J. G. (2003) *Biochemistry* **42,** 1508–1516